CONFIDENTIAL

NACA

RESEARCH MEMORANDUM

SMALL-SCALE TRANSONIC INVESTIGATION OF THE EFFECTS OF FULL-SPAN AND PARTIAL-SPAN LEADING-EDGE FLAPS ON THE AERODYNAMIC CHARACTERISTICS OF A 50° 38' SWEPTBACK WING OF ASPECT RATIO 2.98

By Kenneth P. Spreemann and William J. Alford, Jr.

Langley Aeronautical Laboratory
Langley Field, Va.

CLASSIFIED DOCUMENT

NATIONAL ADVISORY COMMITTEE
FOR AERONAUTICS

WASHINGTON
July 16, 1952

CONFIDENTIAL

NATIONAL ADVISORY COMMITTEE FOR AERONAUTICS

RESEARCH MEMORANDUM

SMALL-SCALE TRANSONIC INVESTIGATION OF THE EFFECTS OF FULL-SPAN AND PARTIAL-SPAN LEADING-EDGE FLAPS ON THE AERODYNAMIC CHARACTERISTICS OF A 50° 38' SWEPTBACK WING OF ASPECT RATIO 2.98

By Kenneth P. Spreemann and William J. Alford, Jr.

SUMMARY

A small-scale investigation of the effects of full-span and partial-span leading-edge flaps on the aerodynamic characteristics of a swept-back wing was made in the Langley high-speed 7- by 10-foot tunnel over a Mach number range of 0.70 to 1.10. The basic semispan wing employed in this investigation had the quarter-chord line sweptback 50° 38', aspect ratio 2.98, taper ratio 0.45, and NACA 64A-series airfoil sections tapered in thickness ratio. Lift, drag, pitching moment, and bending moment were obtained for the basic wing (no leading-edge-flap deflection) and for the wing with full-span and partial-span (outboard 55 percent of the semispan) leading-edge-flap deflections of approximately 3°, 6°, and 9°.

The results show that of the leading-edge-flap deflections investigated, 6.0° for the full-span flap and 3.3° for the partial-span flap gave the greatest increases in maximum lift-drag ratios up to Mach number 0.90. Above Mach number 0.90, all leading-edge-flap deflections reduced the maximum lift-drag ratios below those of the basic wing. None of the leading-edge flaps employed was as effective as the warped wing reported in NACA RM L51C16, which maintained maximum lift-drag ratios higher than those of the basic wing throughout the Mach number range investigated. At subsonic Mach numbers the 3° and 6° leading-edge-flap deflections slightly improved the pitch characteristics over those of the basic wing in the high-lift range. No significantly large changes in lift-curve slope or movement of the aerodynamic-center location were occasioned by use of any of the leading-edge-flap deflections; however, there were noticeable increases in minimum drag coefficients above a Mach number of about 0.90.

INTRODUCTION

A number of experimental investigations of warped wings (refs. 1, 2, and 3) have indicated that properly designed twist and camber for a given set of parameters (sweep angle, design lift coefficient, and Mach number) can provide large increases in lift-drag ratios. Since the use of twist and camber presents some structural problems, interest has been shown in the possibility of improving performance characteristics by using moderate leading-edge-flap deflections. Leading-edge-flap deflections were shown to be rather effective in improving the lift-drag ratios of a thin straight wing up to high subsonic speeds (ref. 4). Devices of this nature on a swept wing might conceivably produce improvements in the aerodynamic characteristics similar to those provided by twist and camber. The use of leading-edge flaps also would seem to provide an advantage over twist and camber in that they could readily be altered after completion of an airplane or adapted to existing wings without imposing limitations on possible changes of other components of the wing, such as the ailerons or trailing-edge flaps. Moreover, the leading-edge-flap angle could be varied in flight to give optimum performance for the airplane.

The present investigation was made to determine the effects of full-span and partial-span leading-edge flaps on the aerodynamic characteristics of a sweptback wing. The basic flat wing of reference 1, which had 50° 38' sweepback of the quarter-chord line and aspect ratio 2.98, was employed in this investigation. All leading-edge flaps had chords of 30 percent of the streamwise wing chord. Lift, drag, pitching moment, and bending moment were obtained for the basic wing (no leading-edge-flap deflection) and for the wing with full-span and partial-span leading-edge flap deflections of approximately 3°, 6°, and 9°. This investigation was made in the Langley high-speed 7- by 10-foot tunnel over a Mach number range of 0.70 to 1.10.

COEFFICIENTS AND SYMBOLS

C_L lift coefficient, Twice semispan lift/qS

C_D drag coefficient, Twice semispan drag/qS

C_m pitching-moment coefficient referred to $0.25\bar{c}$, Twice semispan pitching moment/$qS\bar{c}$

C_B bending-moment coefficient about axis parallel to relative wind and in plane of symmetry, Root bending moment/$q \frac{S}{2} \frac{b}{2}$

q effective dynamic pressure over span of model, $\frac{1}{2}\rho V^2$, lb/sq ft

S twice wing area of semispan model, 0.125 sq ft

$\bar{c}$ mean aerodynamic chord of wing, 0.215 ft, $\frac{2}{S}\int_0^{b/2} c^2 dy$ (using theoretical tip, see fig. 1)

c local wing chord parallel to plane of symmetry, ft

b twice span of semispan model, 0.61 ft

y spanwise distance from plane of symmetry, ft

ρ air density, slugs/cu ft

V effective stream velocity over model, fps

M effective Mach number, $\frac{2}{S}\int_0^{b/2} cM_a \, dy$

M_a average chordwise Mach number

M_l local Mach number

R Reynolds number, $\frac{\rho V \bar{c}}{\mu}$

μ absolute viscosity, lb-sec/sq ft

α angle of attack of wing chord plane, deg

δ_n leading-edge-flap deflection, deg (measured down from wing chord plane in a plane parallel to the air stream)

y_{cal} lateral center of additional loading, $100 \frac{\partial C_B}{\partial C_L}$, percent semispan

C_{m_0} pitching-moment coefficient at zero lift coefficient

$C_{D_{min}}$ minimum drag coefficient

$C_{L_{C_{D_{min}}}}$ lift coefficient at minimum drag coefficient

$(L/D)_{max}$ maximum lift-drag ratio

$\left[\frac{(L/D)_{max_{\delta_n}}}{(L/D)_{max\ \delta_{n=0}}}\right]$ performance ratio - maximum lift-drag ratio of wing with flaps deflected referred to the maximum lift-drag ratio of the basic wing

$C_{L(L/D)_{max}}$ lift coefficient at maximum lift-drag ratio

MODELS AND APPARATUS

The semispan steel wing employed in this investigation had 50° 38' sweepback of the quarter-chord line, aspect ratio 2.98, and taper ratio of 0.45. The wing had an NACA $64_{(10)}$A010.9 airfoil section at the root and an NACA $64_{(08)}$A008.1 at the tip measured perpendicular to the 29.3-percent-chord line. A drawing of the model, including the three full-span-flap deflections, is shown in figure 1. A photograph of a typical sweptback-wing model mounted on the reflection-plane setup in the Langley high-speed 7- by 10-foot tunnel is shown in figure 2.

The partial-span flap extended over the outboard 55 percent of the semispan. The flap line was established along the 30-percent-streamwise-chord line by means of a groove of $\frac{1}{32}$-inch width and about half the depth of the local section. The flap angles were set by bending the leading-edge segment of the wing about this groove. After setting the flap angle desired, the groove was filled and finished off flush with the wing surface. Angular distortion of the flap under load was negligible.

Force and moment measurements were made with a strain-gage-balance system and recorded with recording potentiometers. The angle of attack was measured by means of a slide-wire potentiometer and recorded with a recording potentiometer.

TESTS

The investigation was made in the Langley high-speed 7- by 10-foot tunnel with the model mounted on a reflection plane (fig. 1) located approximately $3\frac{1}{4}$ inches from the tunnel wall in order to bypass the wall boundary layer. The reflection-plane boundary-layer thickness was such that a value of 95 percent of free-stream velocity was reached at a distance of approximately 0.16 inch from the surface of the reflection plane for all test Mach numbers. This boundary-layer thickness represented a distance of about 4.5 percent semispan for the model tested.

At Mach numbers below 0.93, there was practically no velocity gradient in the vicinity of the reflection plane. At higher Mach numbers, however, the presence of the reflection plane created a high-local-velocity field in the vicinity of the reflection plane which permitted testing the small models up to $M = 1.10$ before choking occurred in the tunnel. The variations of local Mach numbers in the region occupied by the models are shown in figure 3. Effective test Mach numbers were obtained from additional contour charts similar to those shown in figure 3 by the relationship $M = \frac{2}{S}\int_0^{b/2} cMa\ dy$.

For the model tested, Mach number variations (outside the boundary layer) of less than 0.01 over the surface of the model generally were obtained below $M = 0.95$. Local Mach number variations of about 0.05 to 0.07 were obtained between $M = 0.98$ to $M = 1.10$. It should be noted that in the investigation of reference 1 in which the transonic-bump technique was employed, the Mach number variations are principally spanwise; whereas in this investigation they are principally chordwise. The dissimilarities in test facilities, Mach number gradients, and effects of the transonic-bump curvature on the effective sweep angle of the model may account for some of the apparently unexplainable differences in the basic-wing results of the two investigations.

A gap of about $\frac{1}{16}$-inch was maintained between the wing-root-chord section and the reflection-plane-plate turntable and a sponge-wiper seal was fastened to the wing butt behind the turntable to minimize leakage. Force and moment measurements were made for the model over a Mach number range from 0.70 to 1.10 and an angle-of-attack range from -10° to 22°. The full-span-flap deflections were 3.1°, 6.0°, and 9.0° and the partial-span-flap deflections were 3.3°, 6.0°, and 9.0°. The variation of Reynolds number with Mach number for these tests is shown in figure 4.

In view of the small size of the model relative to the tunnel test section, jet-boundary and blockage corrections were believed to be negligible and were not applied to the data. Corrections due to aeroelastic effects were less than 1.0 percent and were not applied to the data.

RESULTS AND DISCUSSION

The figures presenting the results are grouped as follows:

	Figures
Basic aerodynamic data	5 to 7
Lift-drag ratios	8 to 10
Summary of aerodynamic characteristics	11 to 12

Unless otherwise noted, the discussion is based on the summary curves presented in figures 11 and 12. The slopes presented in these figures have been averaged over a lift-coefficient range of -0.2 to 0.2.

Lift Characteristics

The lift-curve slopes with full-span leading-edge flaps deflected were generally slightly lower than that realized for the basic wing (see fig. 11); only minor differences in the values of lift-curve slope were noted with the partial-span flaps deflected (fig. 12). The variation of lift-curve slope with Mach number was not materially affected by any leading-edge-flap deflection. Parts (a) of figures 5, 6, and 7 show that in the high angle-of-attack range the 3.3° partial-span-flap deflection slightly extended C_L in the lower Mach number range, whereas all the other flap deflections generally gave varying amounts of reductions in C_L.

All leading-edge-flap deflections caused gradual increases in the angle of attack for zero lift $\alpha_{C_{L=0}}$ with Mach number up to $M = 0.95$; above this speed there was little effect of Mach number. The 3.3° partial-span-flap deflection and the wing with partial-span leading-edge camber of reference 5 (which approximated the same equivalent flap deflection) gave negative angles of attack for zero lift below a Mach number of 0.90, whereas all other leading-edge-flap deflections gave positive angles of attack for zero lift throughout the Mach number range investigated. It may also be noted that inconsistencies in relative magnitude of some of the aerodynamic characteristics were indicated; however the general trends attributable to the leading-edge-flap deflections were usually consistent. See, for example, figure 11 in which $\alpha_{C_{L=0}}$ for 3.1° full-span-flap

deflection is slightly higher than for 6.0° full-span-flap deflection but all full-span-flap deflections gave increases in $\alpha_{C_{L=0}}$.

The lateral center of additional loading, y_{cal}, was hardly affected below M = 0.90 by the full-span leading-edge-flap deflections, whereas the partial-span-flap deflections produced inboard shifts of y_{cal} in this Mach number range. Above a Mach number of about 0.95, y_{cal} was moved outboard of that of the basic wing by all flap deflections.

Drag Characteristics

It can be observed in parts (b) of figures 5, 6, and 7 that the 6.0° full-span-flap deflection gave the most favorable drag characteristics of all the flap deflections investigated. Below M = 0.95, the leading-edge flaps caused the drag to be lower for a given C_L in the higher lift range (see parts (b) of figs. 5, 6, and 7). Similar effects were noted for the twisted and cambered wing of reference 1, except in that case, the wing maintained much more favorable drag effects throughout the Mach number range investigated.

The minimum drag coefficient $C_{D_{min}}$ was progressively increased with leading-edge-flap deflection, the greatest increases occurring in the Mach number range between M = 0.95 to 1.10. The minimum drag values presented in this paper for the basic model were considerably higher than the values obtained in reference 1. As previously pointed out these dissimilarities in the resultant data possibly may be attributed to the differences in test facilities, Mach number gradients, and effects of the transonic-bump curvature on the effective sweep angle of the model. The lift coefficient for minimum drag $C_{L_{C_{D_{min}}}}$ ranged between 0.02 and 0.08 for the various flap deflections and generally decreased with increasing Mach number.

Lift-Drag Ratios

An inspection of figures 8, 9, and 10 reveals that in the higher lift range (above C_L = 0.20 to 0.30) all leading-edge-flap deflections gave marked gains in lift-drag ratios up to about M = 0.90. The 6.0° full-span-flap deflection appeared to give the highest and most consistent gains in lift-drag ratios although the 3.3° partial-span-flap deflection was not greatly inferior.

The maximum lift-drag ratios of the configurations with leading-edge flaps deflected have been referred to the maximum lift-drag ratios

of the basic wing to give the performance ratio $\left[\frac{(L/D)_{max_{\delta_n}}}{(L/D)_{max_{\delta_{n=0}}}}\right]$ (see figs. 11 and 12). It is believed that, when comparing performance characteristics of the present configurations with those of reference 1, use of the performance ratio provides a more reliable basis for comparison than could be obtained from the absolute values of $(L/D)_{max}$ because of the differences in $C_{D_{min}}$ values between the two investigations.

The parameter $\left[\frac{(L/D)_{max_{\delta_n}}}{(L/D)_{max_{\delta_{n=0}}}}\right]$ indicates that 6.0° full-span- and 3.3° partial-span-flap deflections gave the greatest increases in $(L/D)_{max}$ up to a Mach number of 0.90 and above this Mach number all flap deflections gave reductions in $(L/D)_{max}$. Similar results in the maximum lift-drag ratios were obtained for the wing-alone configuration of the wing with partial-span leading-edge camber reported in reference 5. The performance ratios for the warped wing of reference 1 were evaluated by referring the minimum drag values of that reference to the minimum drag values of this investigation and are presented in figure 11 for comparison. It is apparent that no leading-edge-flap deflection approached the $(L/D)_{max}$ improvements provided by the warped wing of reference 1, and figure 11 shows that twisting and cambering the wing maintained these gains in $(L/D)_{max}$ throughout the Mach number range investigated.

Pitching-Moment Characteristics

Comparison of the curves of $\frac{\partial C_m}{\partial C_L}$ (figs. 11 and 12) shows that with respect to the basic wing 6.0° full span and 9.0° full span and partial span were the only leading-edge-flap deflections that gave any appreciable variations in the aerodynamic-center location with Mach number. These configurations tended to shift the aerodynamic-center location rearward in the subsonic Mach number range, whereas the other configurations maintained rather constant aerodynamic-center locations up to a Mach number of about 0.95. All configurations, including the basic wing, gave the usual large rearward shift of the aerodynamic-center location in the mixed-flow region associated with the transonic Mach number range. The 3.3° partial-span-flap deflection was the only flap deflection that resulted in any appreciable forward shift of the aerodynamic-center location in the subsonic Mach number range. Similar effects were observed for the wing with partial-span leading-edge camber of reference 5; although in that case, the shift in aerodynamic-center

location was of considerably smaller magnitude than for the 3.3° partial-span-flap deflection of this investigation.

In the subsonic Mach number range at high lift coefficients, the 3° and 6° leading-edge-flap deflections usually gave slightly more stabilizing pitching-moment characteristics than the basic wing (parts (c) of figs. 5 and 6). Improvements of this nature would be of particular significance for the high-lift landing and maneuvering attitudes of an airplane. Although the pitching moment for zero lift C_{m_0} was changed for each flap deflection investigated, the variations with Mach number were negligible for all the leading-edge-flap deflections; therefore, trim changes affected by a fixed leading-edge-flap deflection would be rather small.

CONCLUSIONS

An investigation of the effects of full-span and partial-span leading-edge-flap deflections of approximately 3°, 6°, and 9° on the aerodynamic characteristics of a sweptback wing indicates the following conclusions:

1. The 6.0° full-span- and 3.3° partial-span-flap deflections gave the greatest increases in maximum lift-drag ratio $(L/D)_{max}$ up to Mach number 0.90. Above a Mach number of 0.90 all leading-edge-flap deflections reduced $(L/D)_{max}$ below that of the basic wing.

2. None of the leading-edge flaps employed was as effective as the warped wing of NACA RM L51C16, which maintained higher $(L/D)_{max}$ values than the basic wing throughout the Mach number range investigated.

3. The 3° and 6° leading-edge-flap deflections slightly improved the pitch characteristics over those of the basic wing in the high-lift range at subsonic Mach numbers.

4. In comparison with the basic wing no significantly large changes in the lift-curve slope or the location of the aerodynamic center were occasioned by any leading-edge-flap deflection; however, there was a noticeable increase in minimum drag coefficient above a Mach number of 0.90.

Langley Aeronautical Laboratory
National Advisory Committee for Aeronautics
Langley Field, Va.

REFERENCES

1. Spreemann, Kenneth P., and Alford, William J., Jr.: Investigation of Effects of Twist and Camber on the Aerodynamic Characteristics of a 50° 38' Sweptback Wing of Aspect Ratio 2.98. Transonic-Bump Method. NACA RM L51C16, 1951.

2. Spreemann, Kenneth P., and Alford, William J., Jr.: Small-Scale Transonic Investigation of the Effects of Twist and Camber on the Aerodynamic Characteristics of a 60° 42' Sweptback Wing of Aspect Ratio 1.94. NACA RM L51I21, 1952.

3. Johnson, Ben H., Jr., and Shibata, Harry H.: Characteristics Throughout the Subsonic Speed Range of a Plane Wing and of a Cambered and Twisted Wing, Both Having 45° of Sweepback. NACA RM A51D27, 1951.

4. Johnson, Ben H., Jr, and Reed, Verlin D.: Investigation of a Thin Wing of Aspect Ratio 4 in the Ames 12-Foot Pressure Wind Tunnel. IV - The Effect of a Constant-Chord Leading-Edge Flap at High Subsonic Speeds. NACA RM A8K19, 1949.

5. Alford, William J., Jr., and Byrnes, Andrew L., Jr.: Small-Scale Transonic Investigation of the Effects of Partial-Span Leading-Edge Camber on the Aerodynamic Characteristics of a 50° 38' Sweptback Wing of Aspect Ratio 2.98. NACA RM L52D08a, 1952.

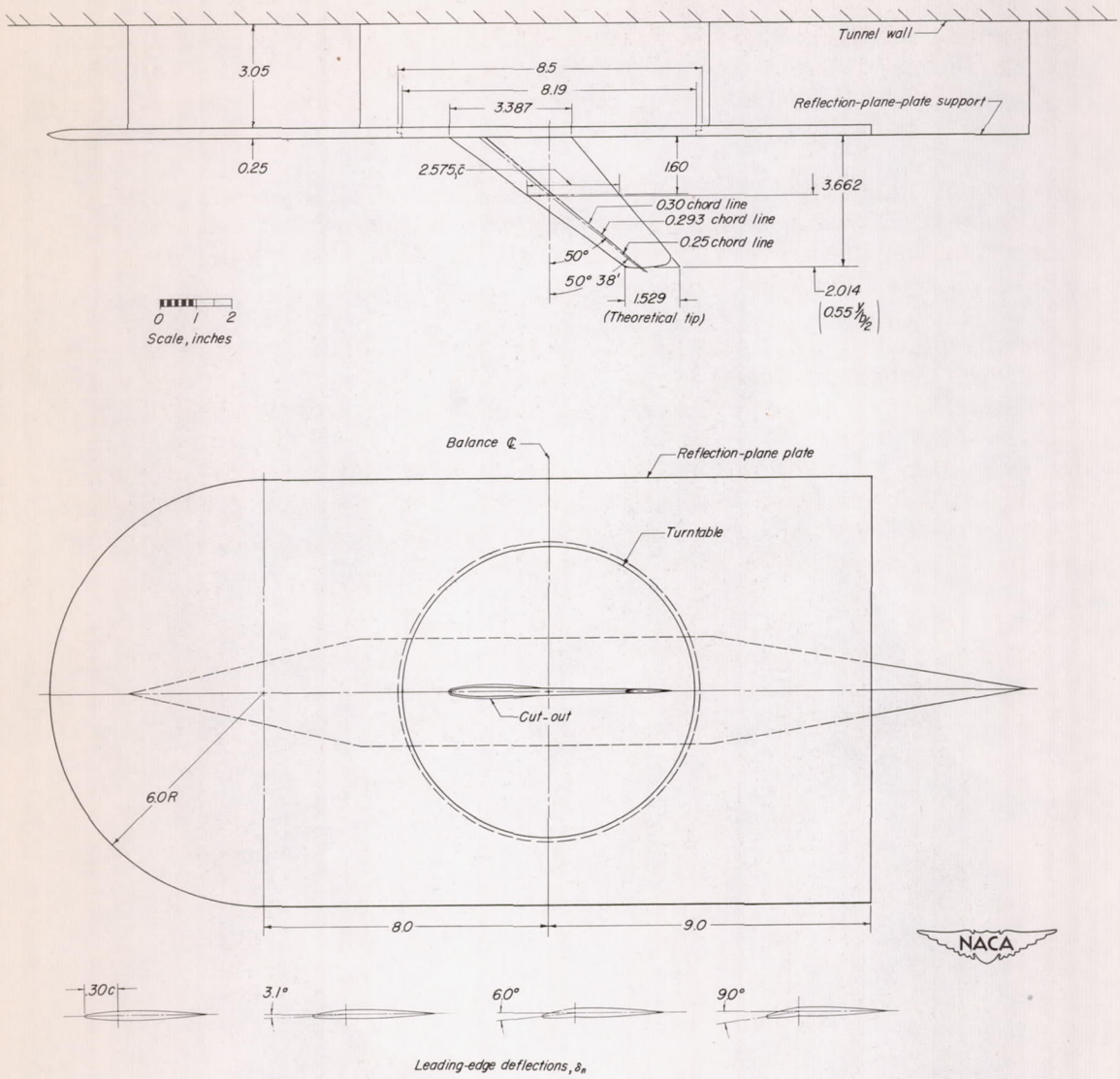

Figure 1.- Test model with 50° 38' sweepback, aspect ratio 2.98, taper ratio 0.45, and modified NACA 64A-series airfoil sections (included are three leading-edge-flap deflections).

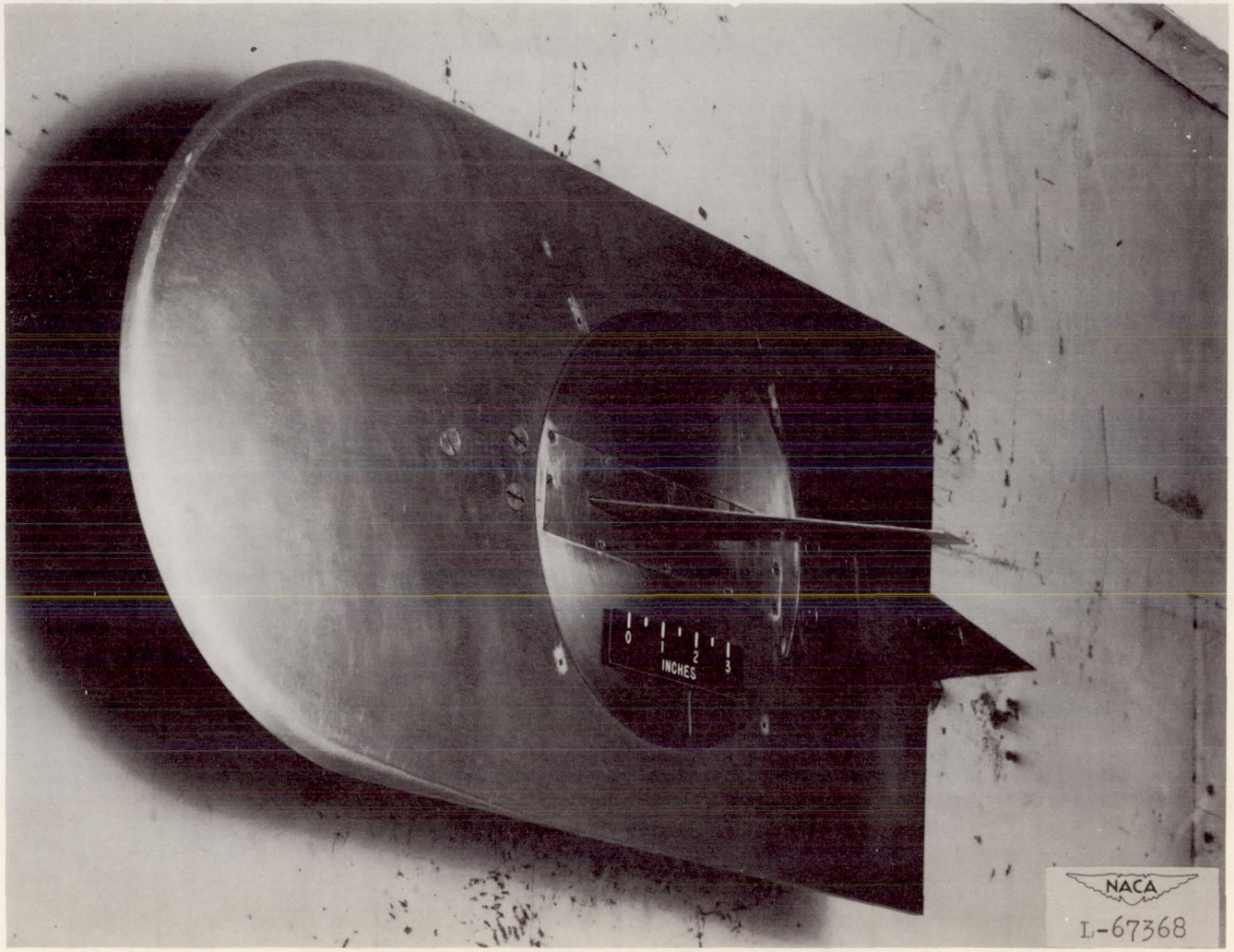

Figure 2.- View of typical model mounted on the reflection plane in the 7- by 10-foot high-speed tunnel.

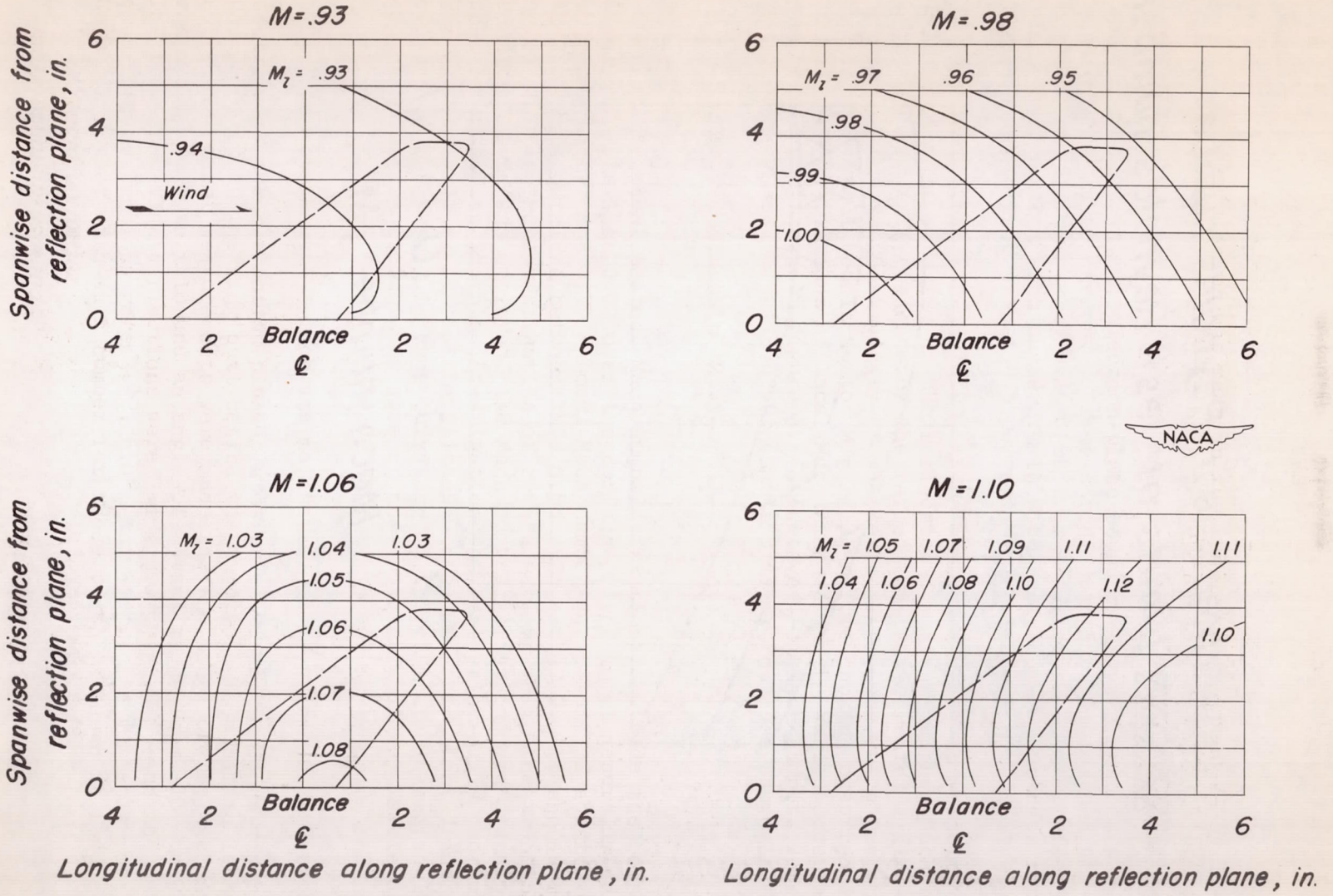

Figure 3.- Typical Mach number contours over reflection plane in region of model location.

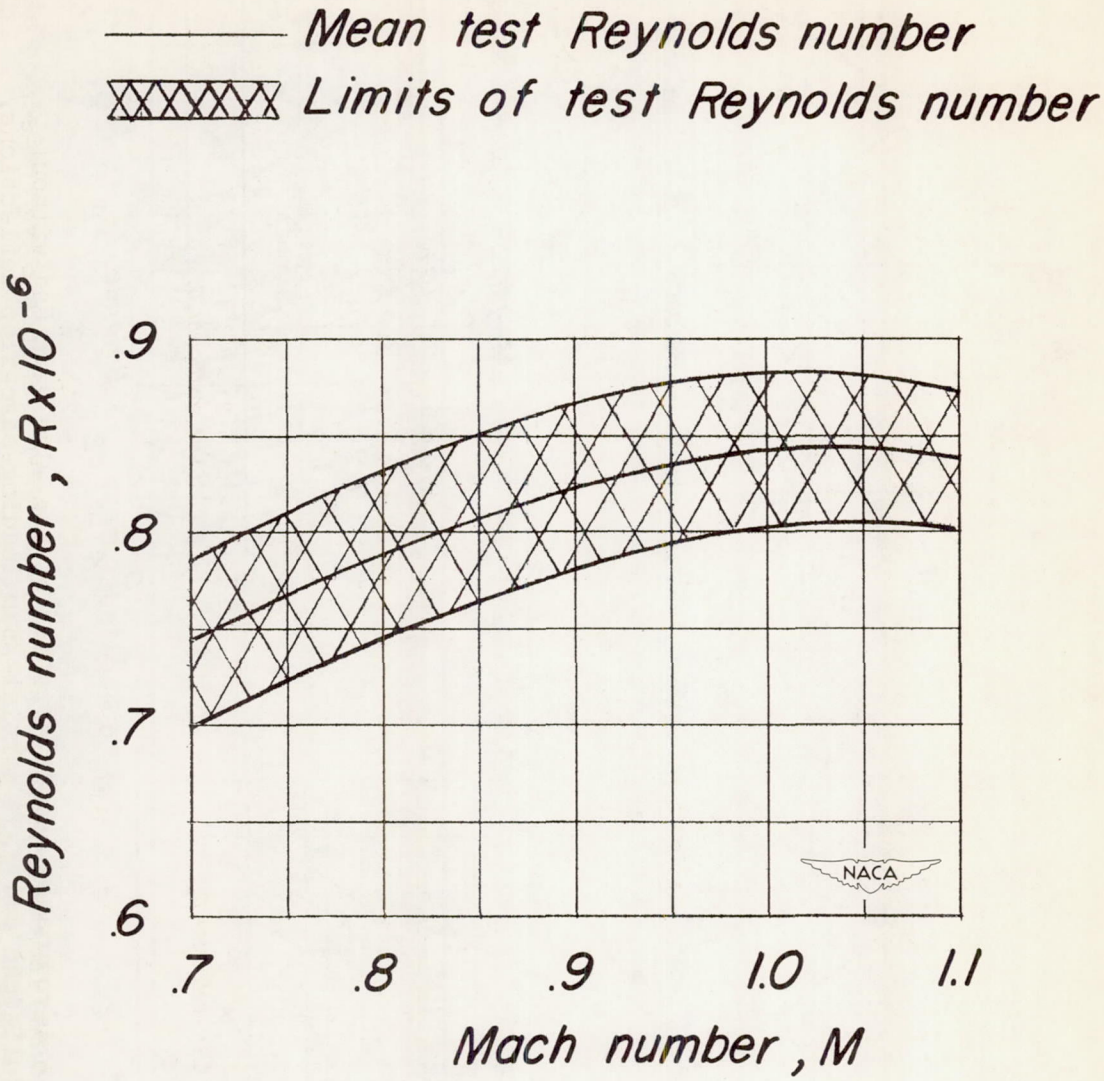

Figure 4.- Variation of test Reynolds number with Mach number.

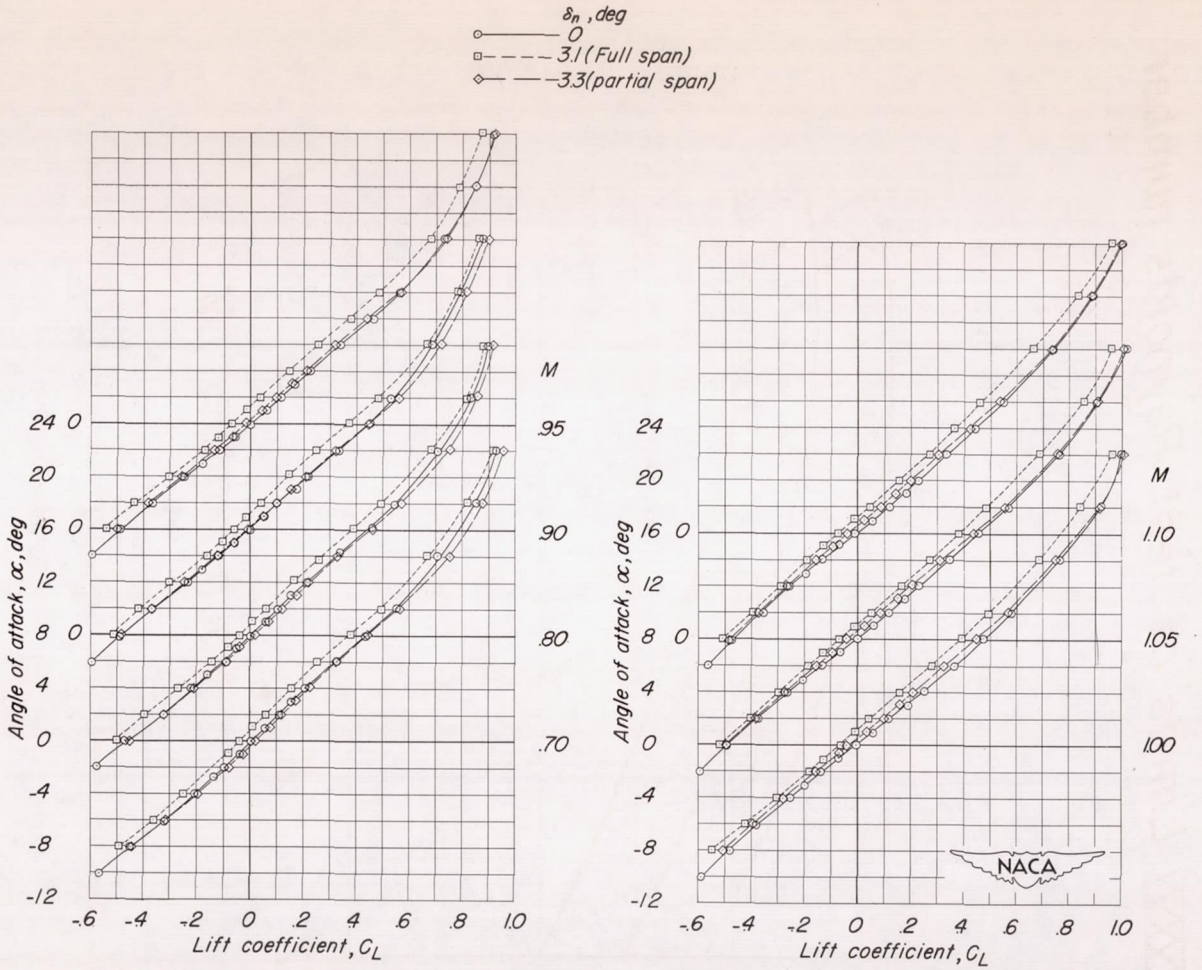

(a) α against C_L.

Figure 5.- Aerodynamic characteristics of the wing with and without 3.1° full-span and 3.3° partial-span leading-edge-flap deflections.

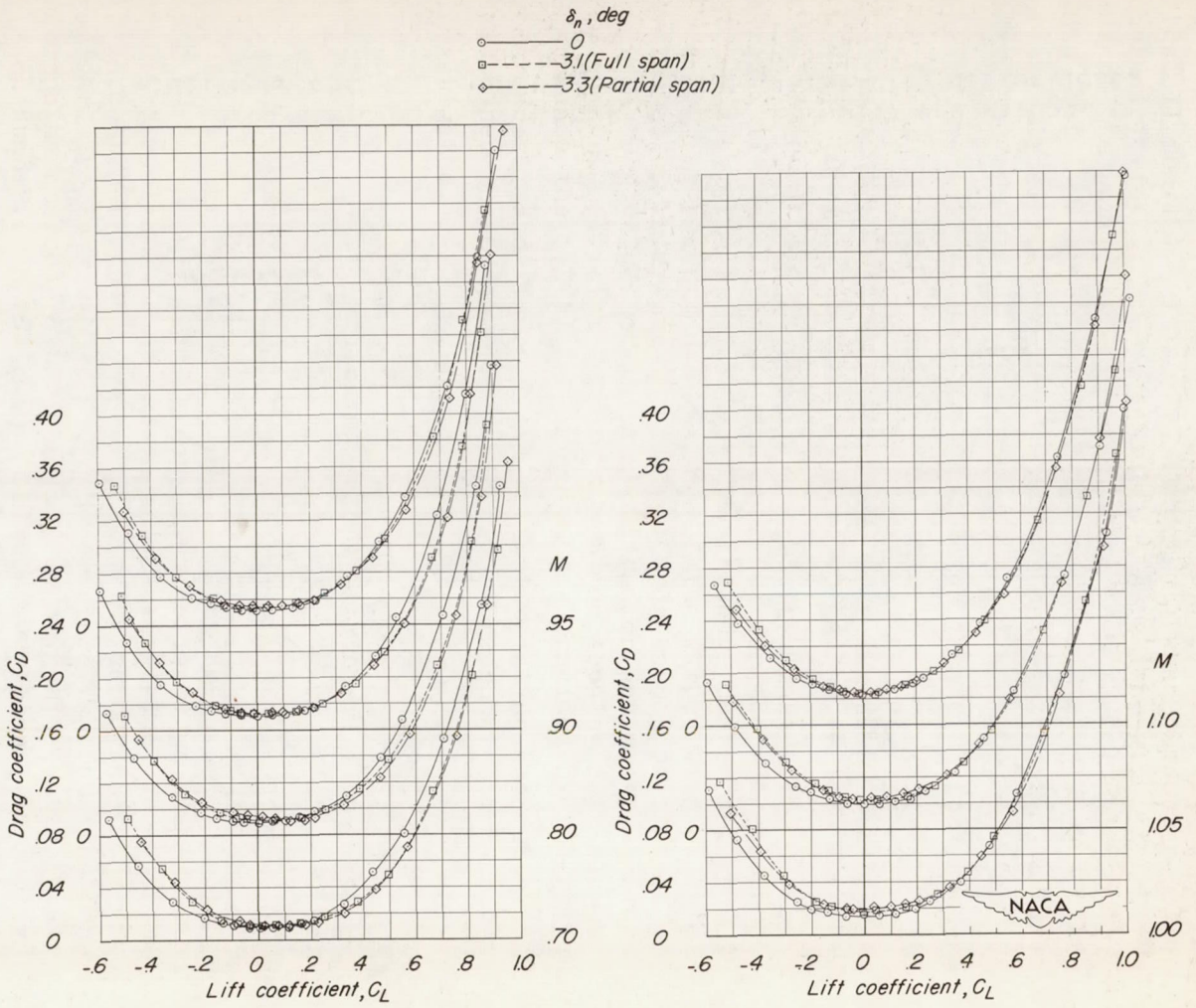

(b) C_D against C_L.

Figure 5.- Continued.

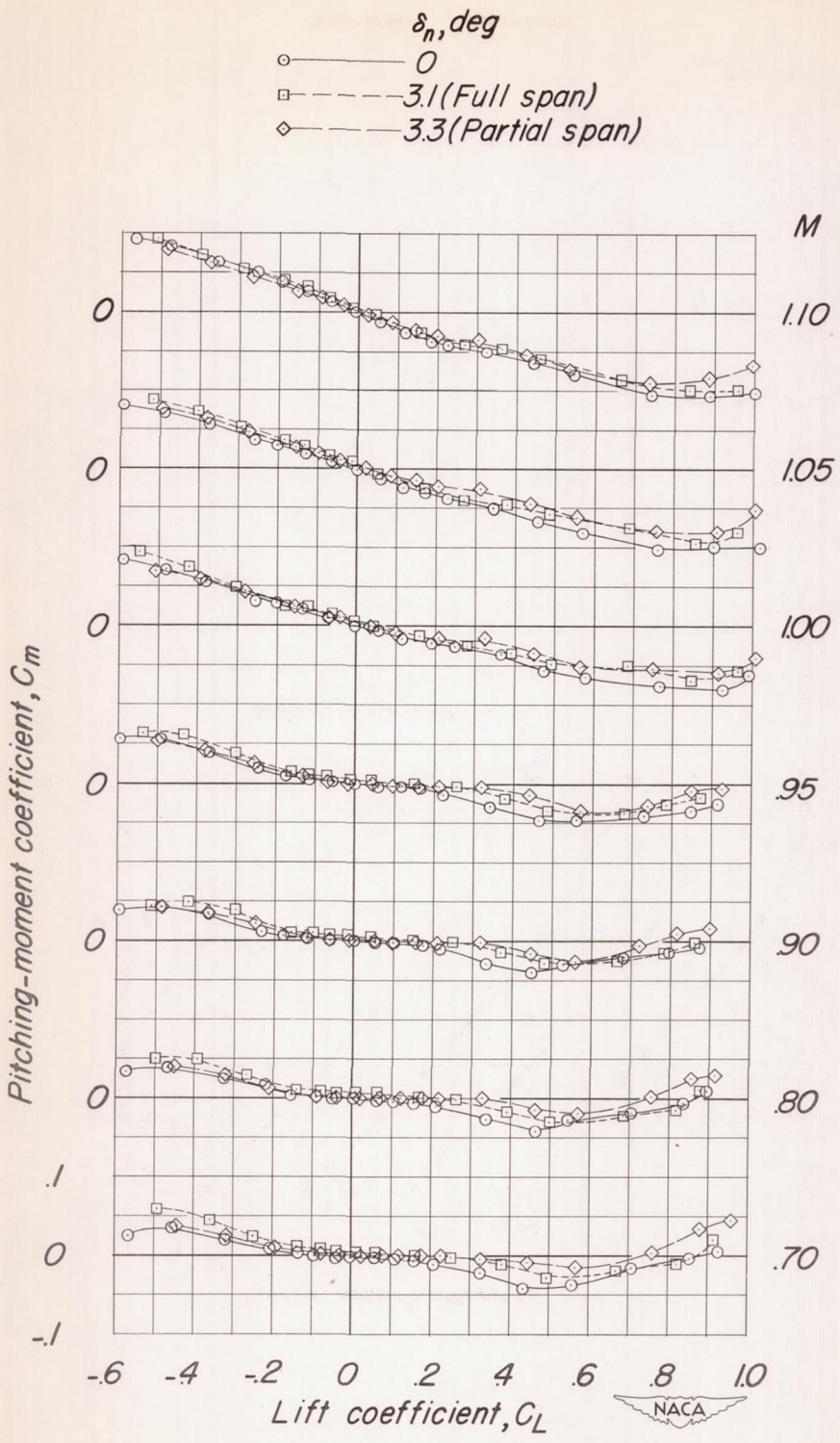

(c) C_m against C_L.

Figure 5.- Continued.

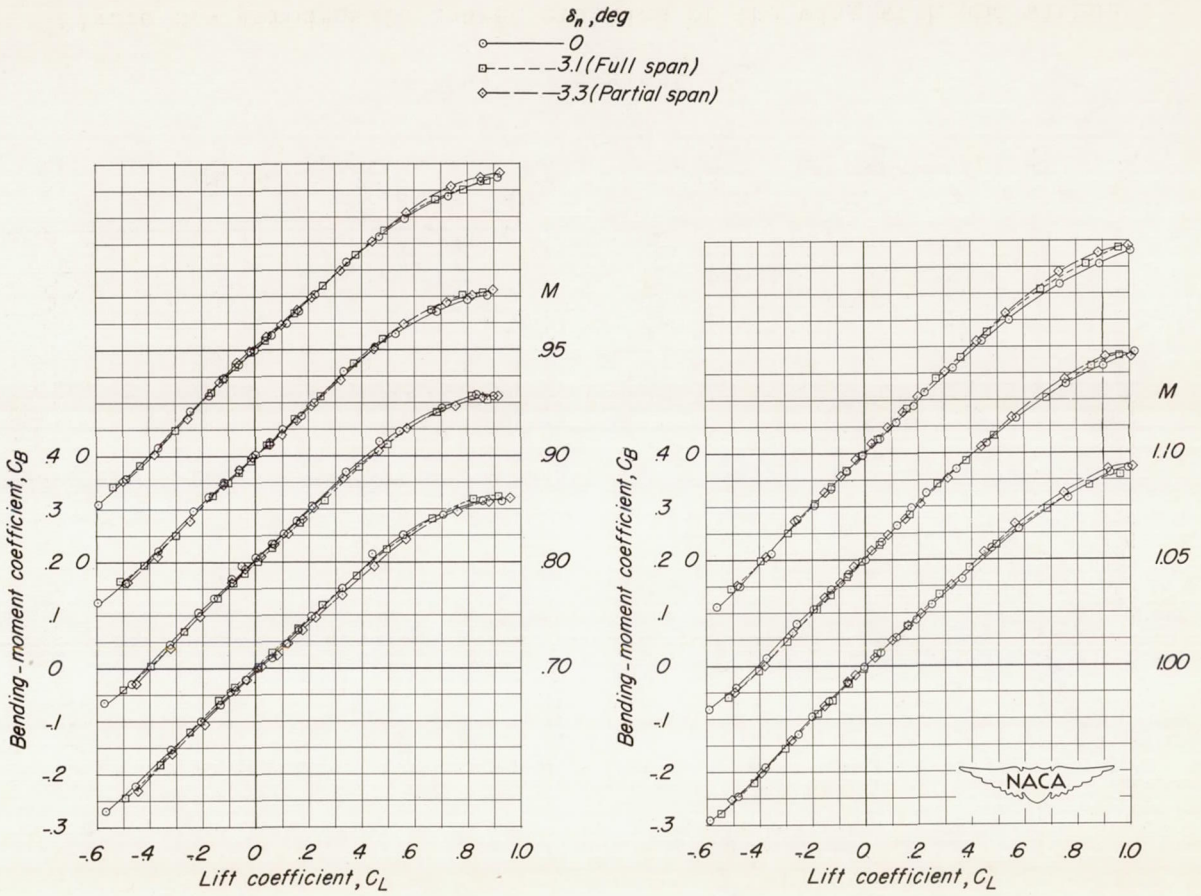

(d) C_B against C_L.

Figure 5.- Concluded.

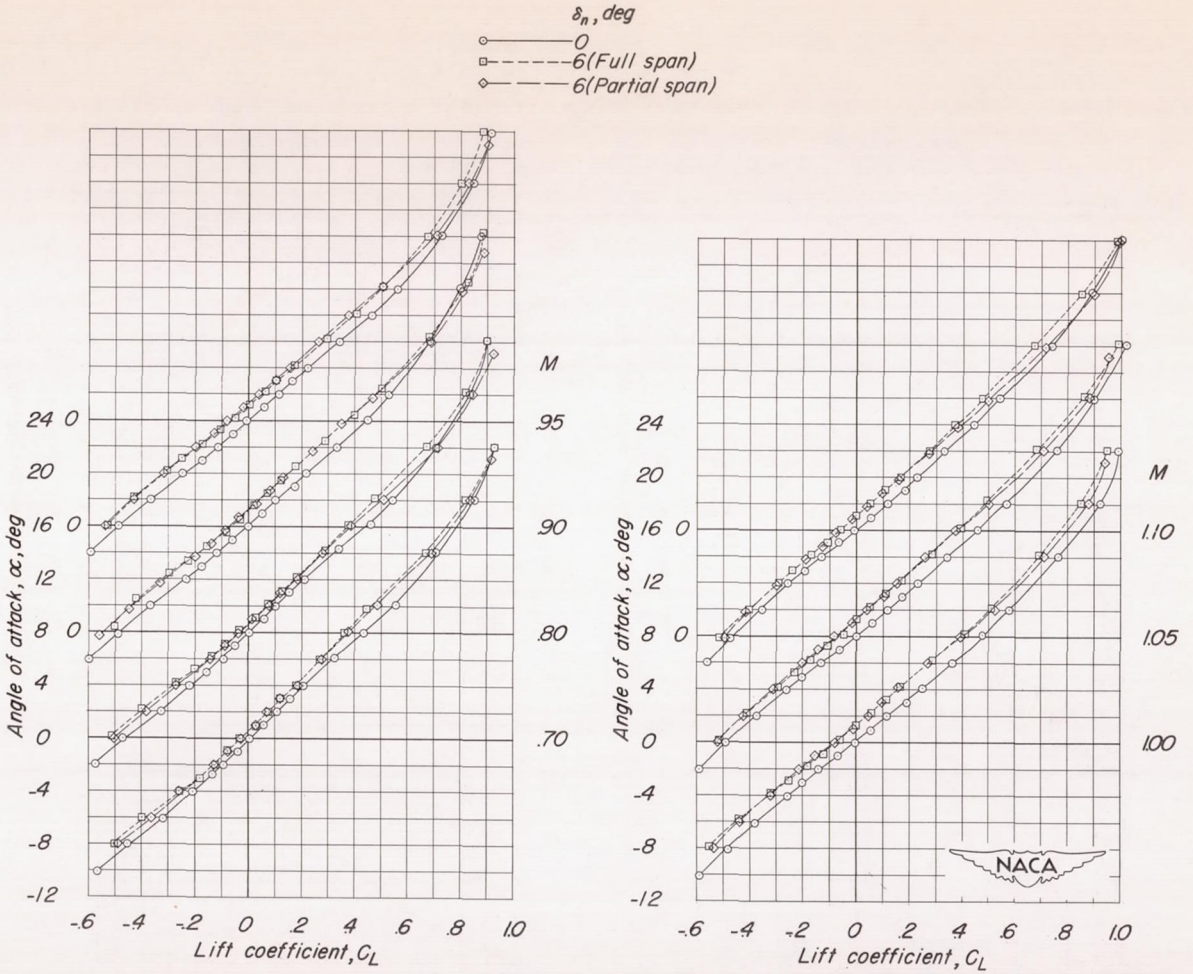

(a) α against C_L.

Figure 6.- Aerodynamic characteristics of the wing with and without 6.0° full-span and partial-span leading-edge-flap deflections.

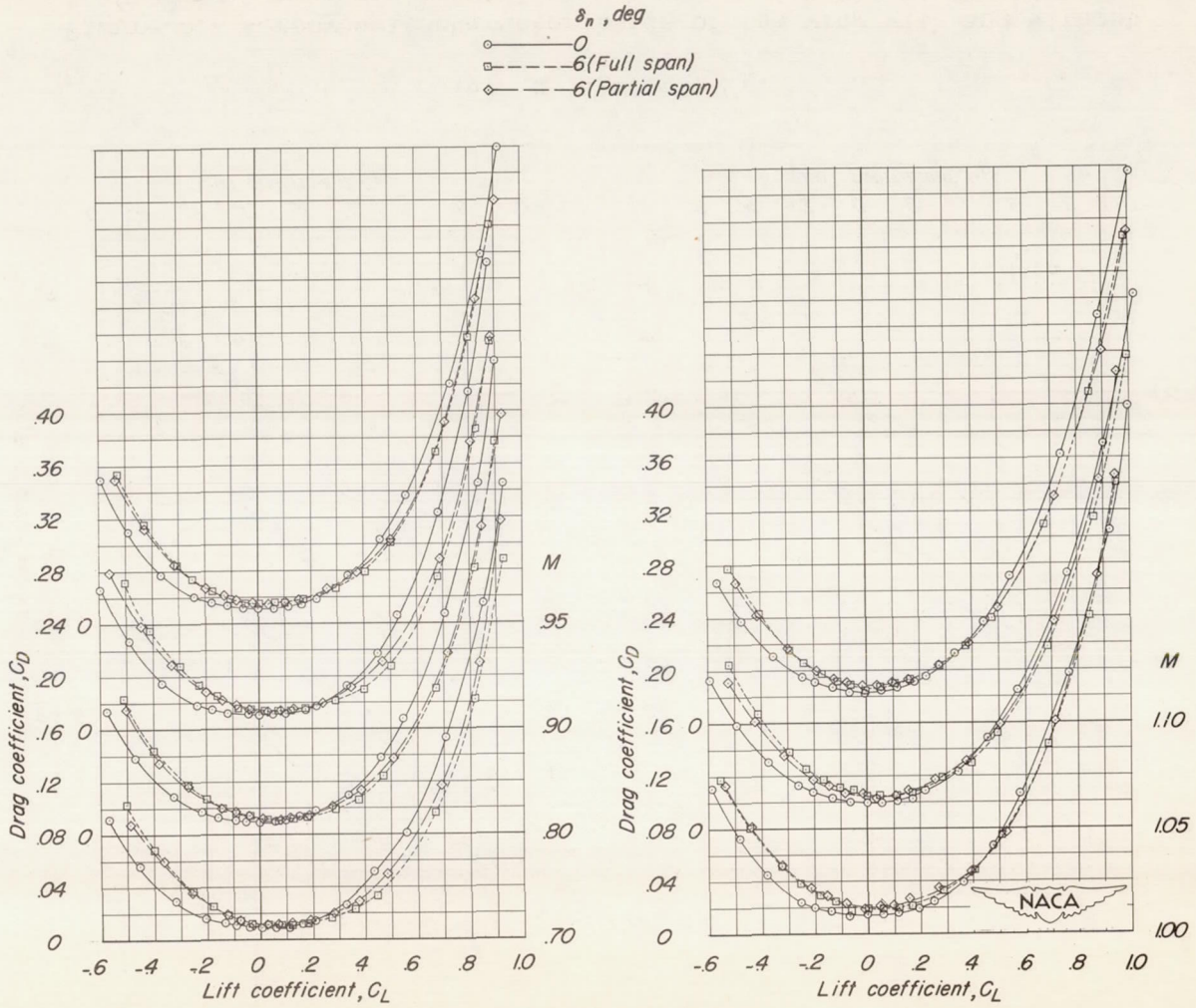

(b) C_D against C_L.

Figure 6.- Continued.

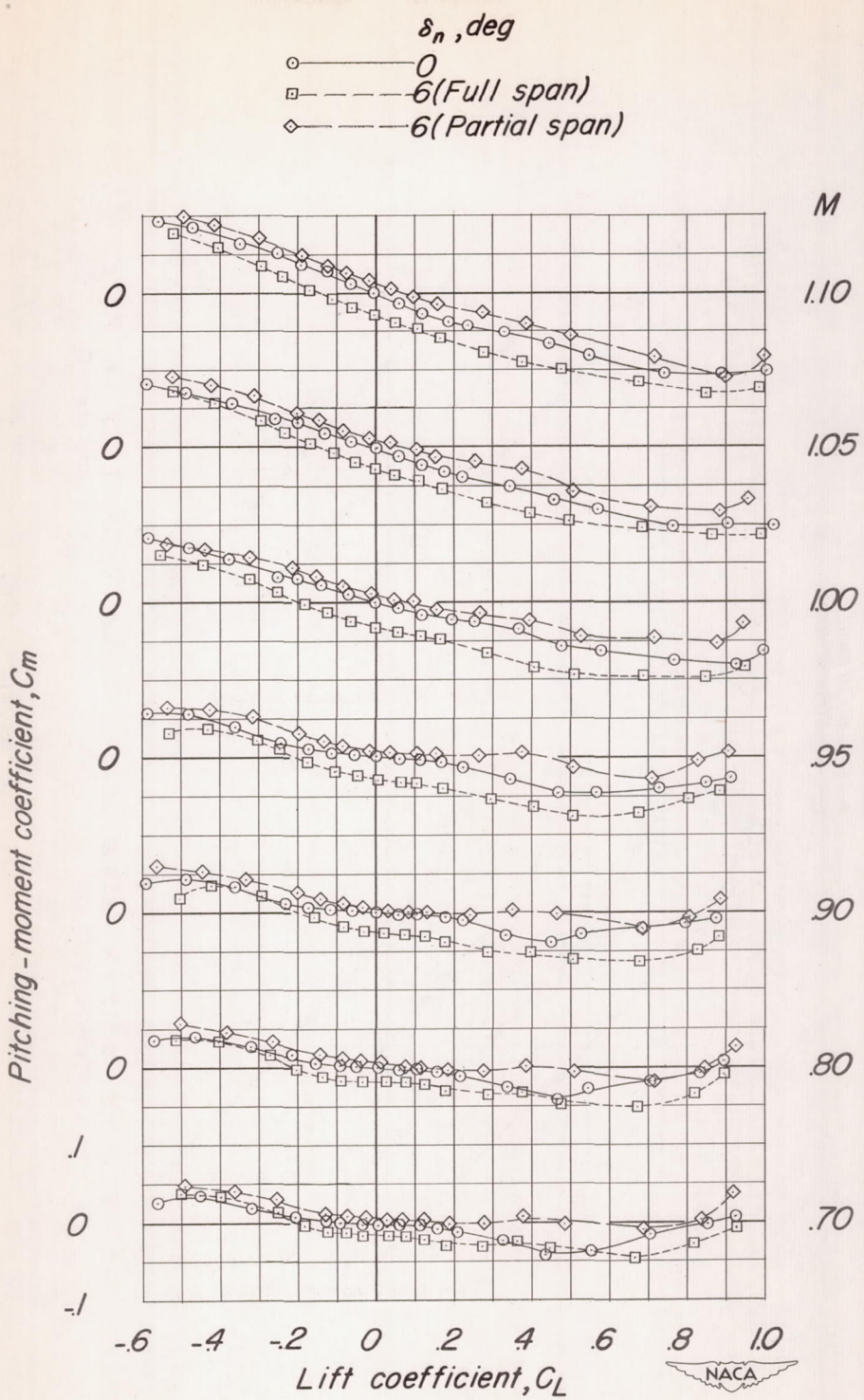

(c) C_m against C_L.

Figure 6.- Continued.

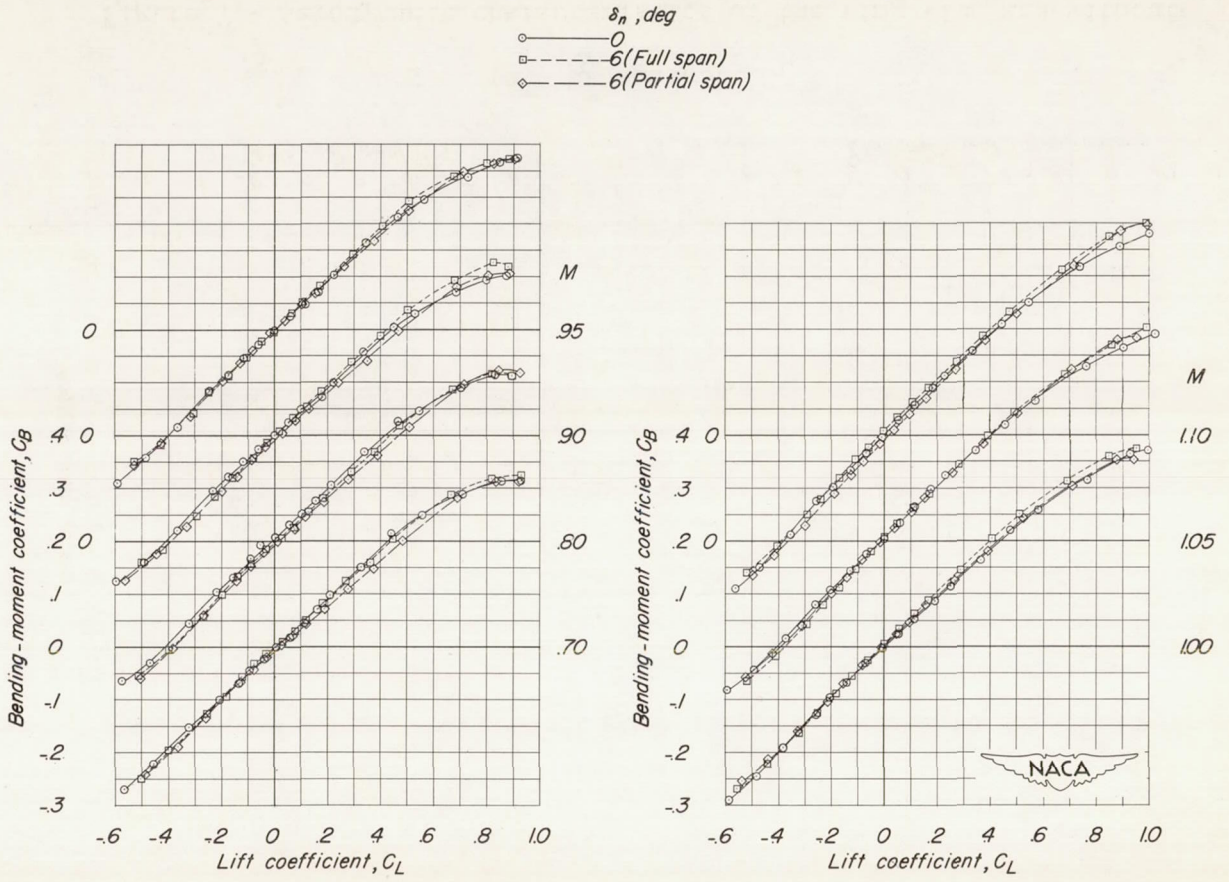

(d) C_B against C_L.

Figure 6.- Concluded.

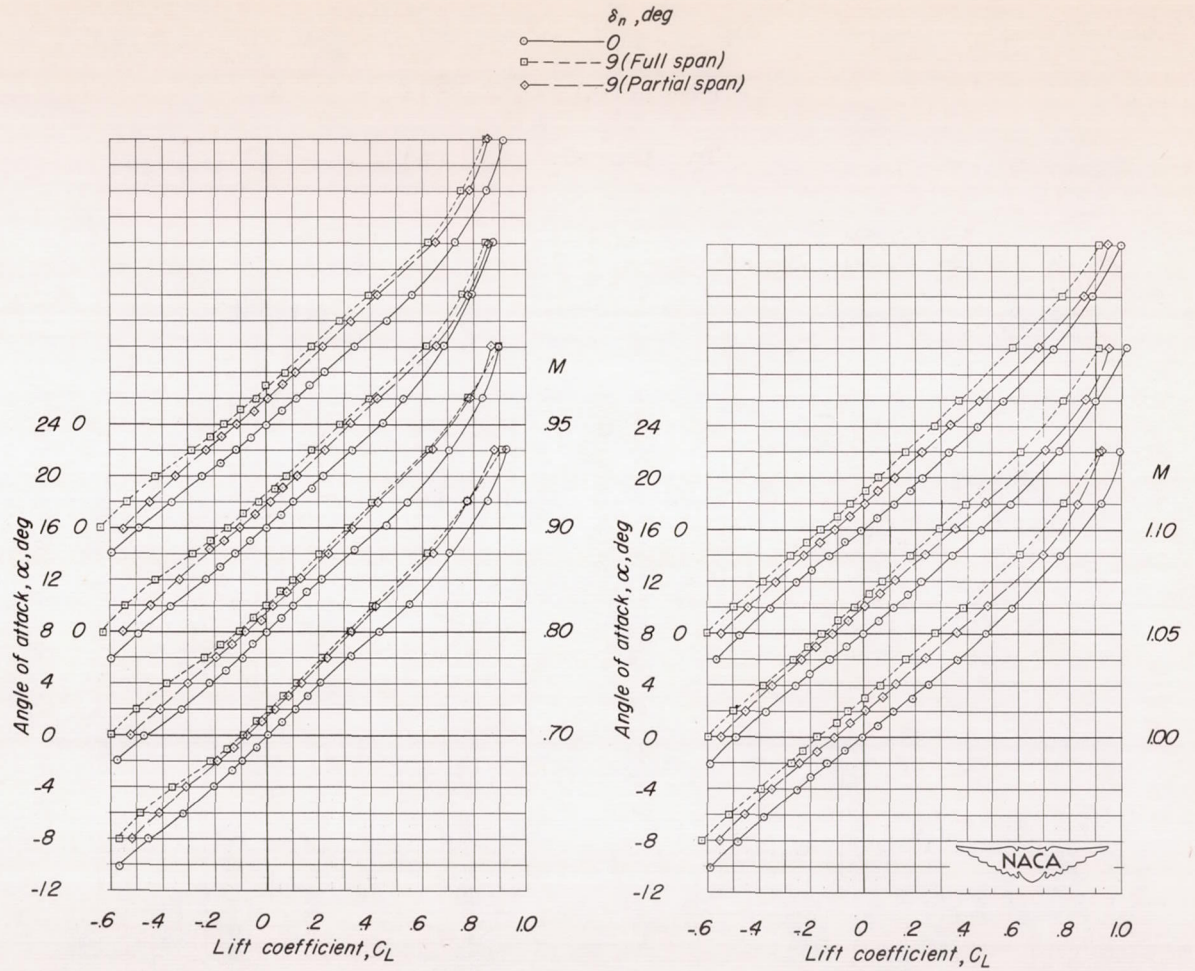

(a) α against C_L.

Figure 7.- Aerodynamic characteristics of the wing with and without 9.0° full-span and partial-span leading-edge-flap deflections.

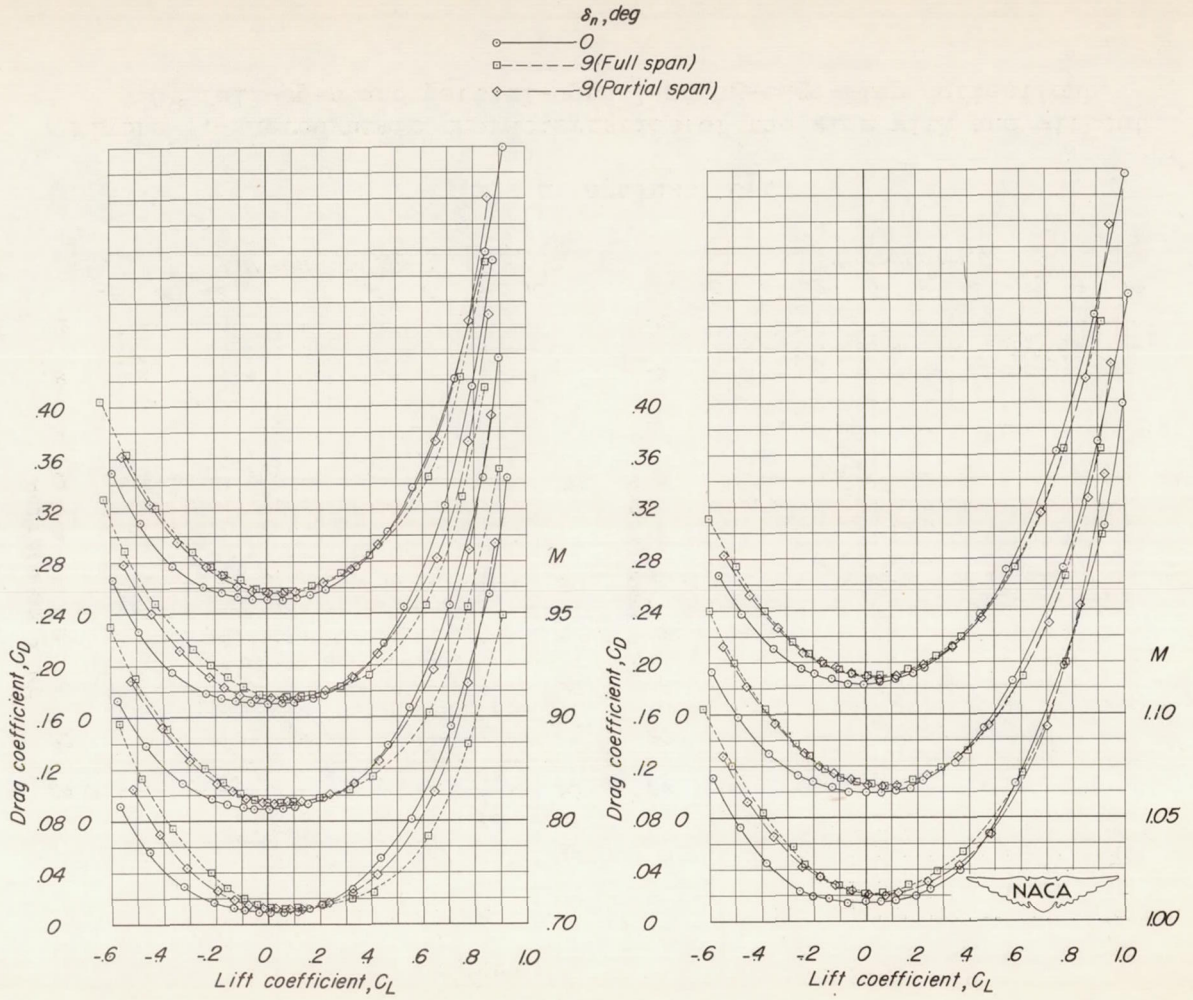

(b) C_D against C_L.

Figure 7.- Continued.

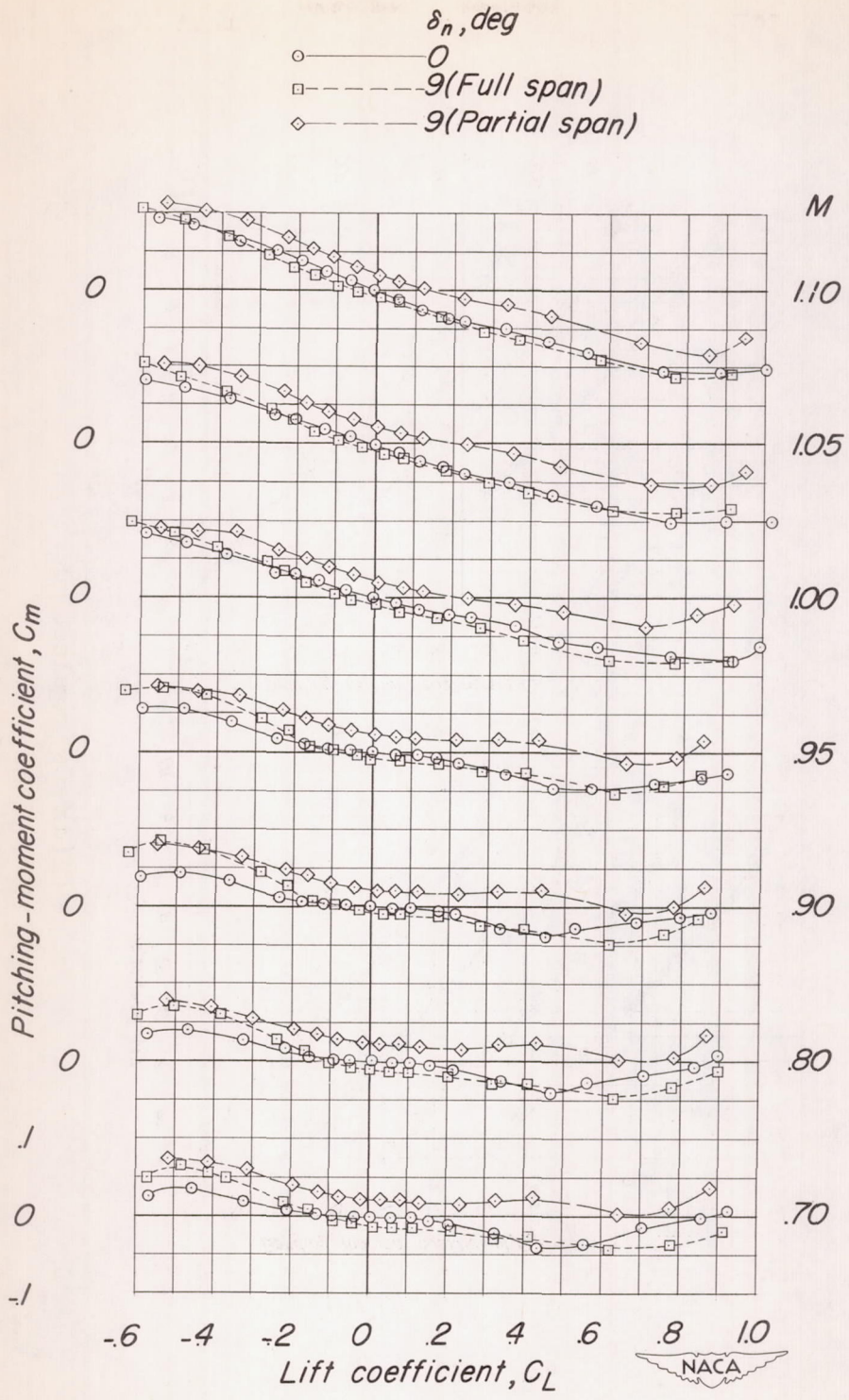

(c) C_m against C_L.

Figure 7.- Continued.

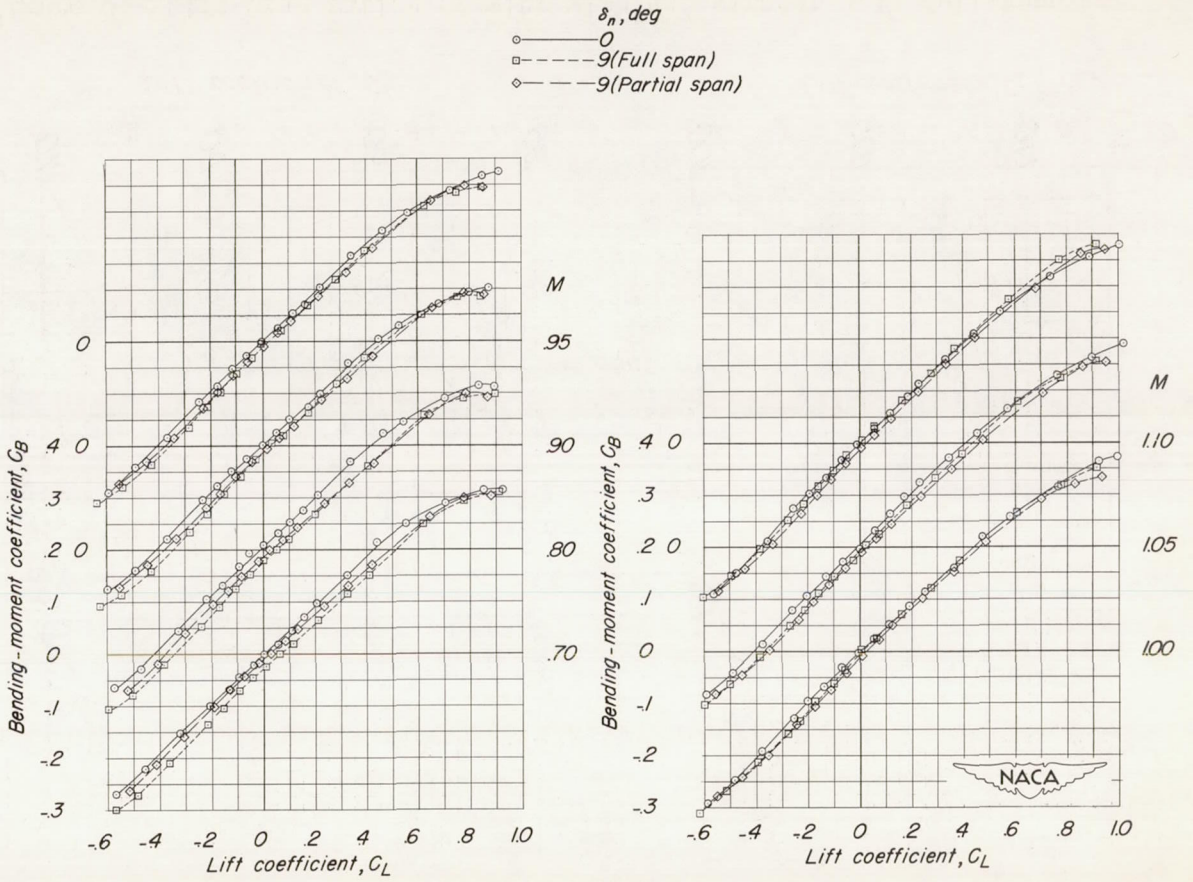

(d) C_B against C_L.

Figure 7.- Concluded.

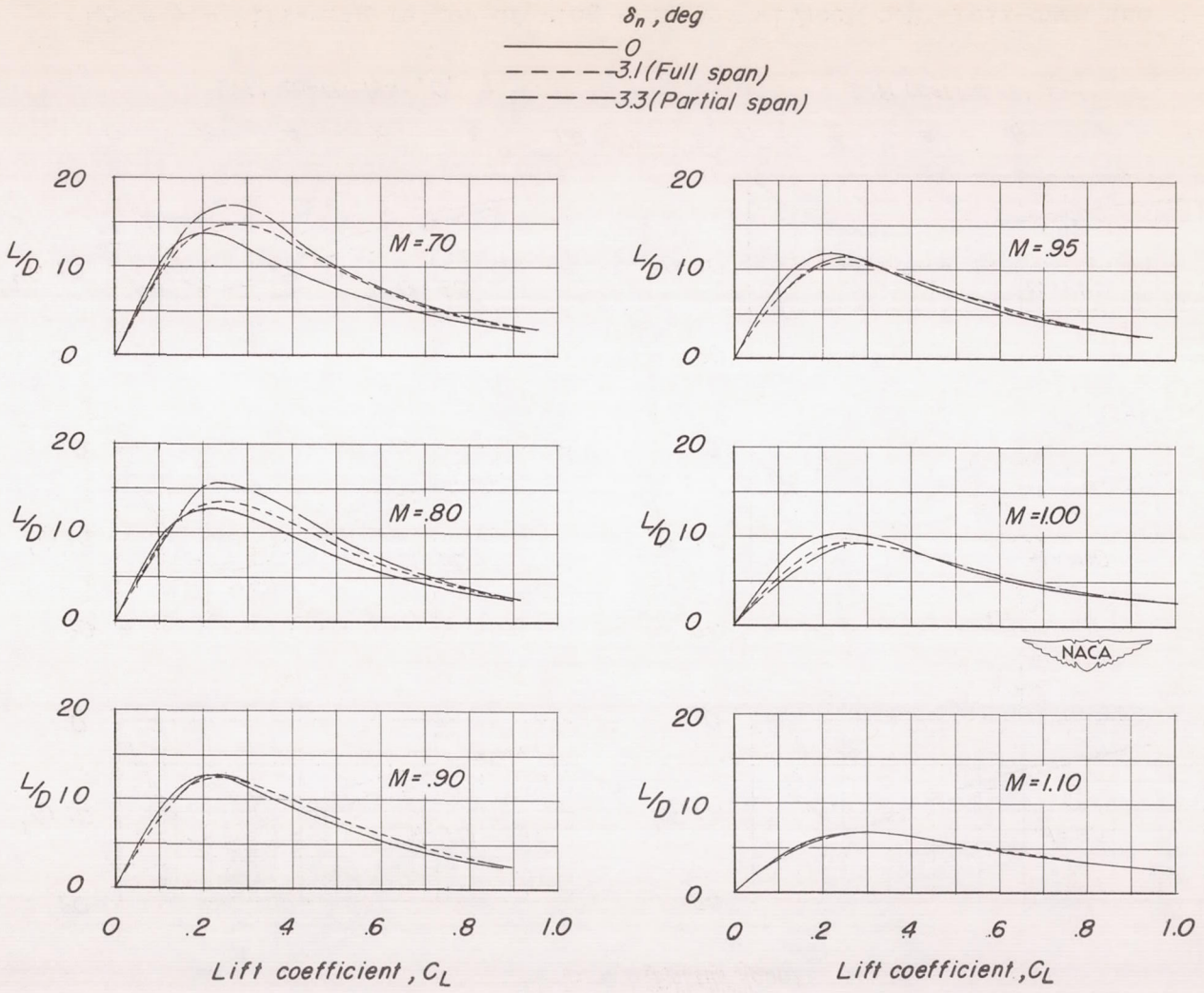

Figure 8.- Lift-drag ratios of wing with and without 3.1° full-span and 3.3° partial-span leading-edge-flap deflections.

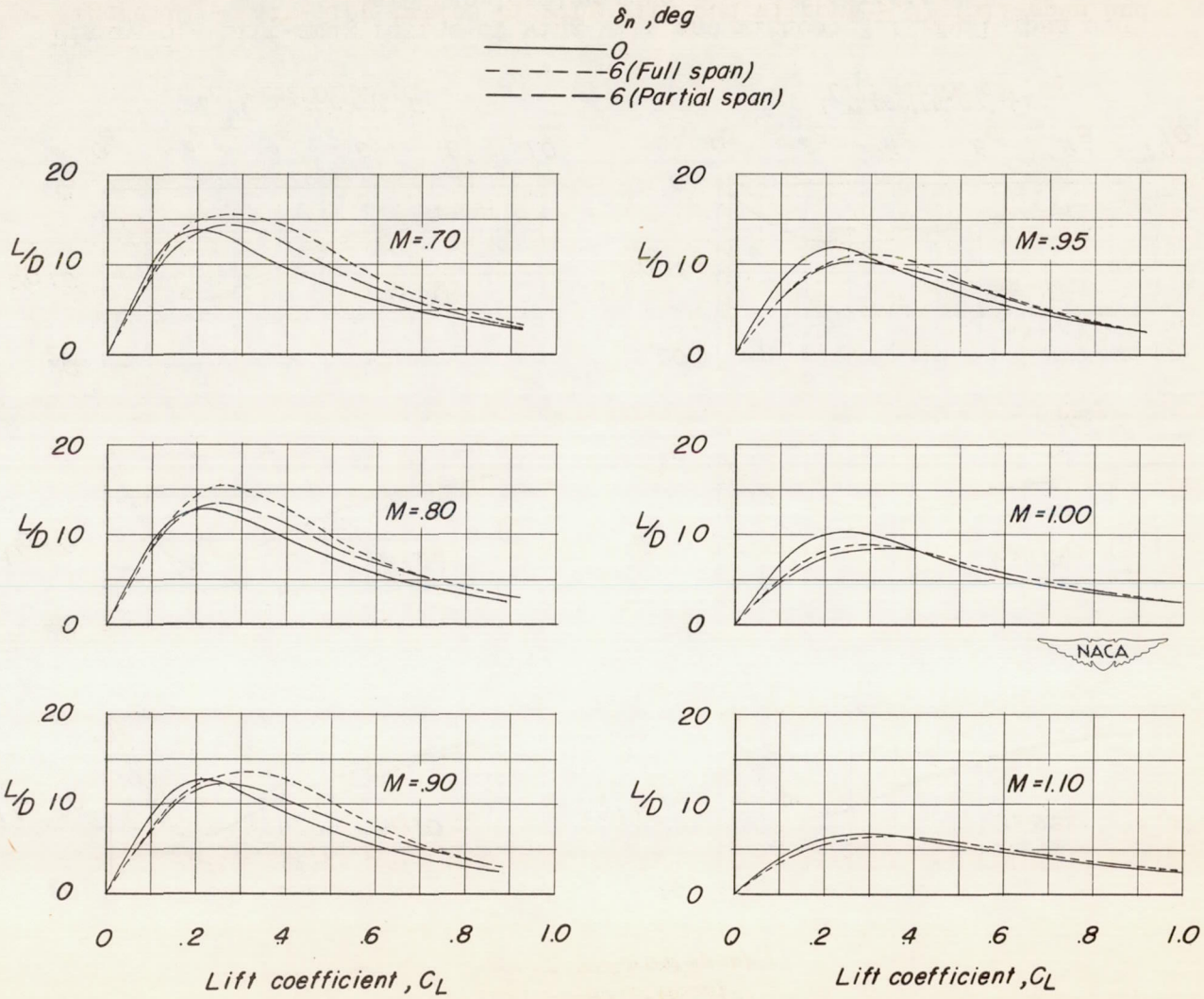

Figure 9.- Lift-drag ratios of wing with and without 6.0° full-span and partial-span leading-edge-flap deflections.

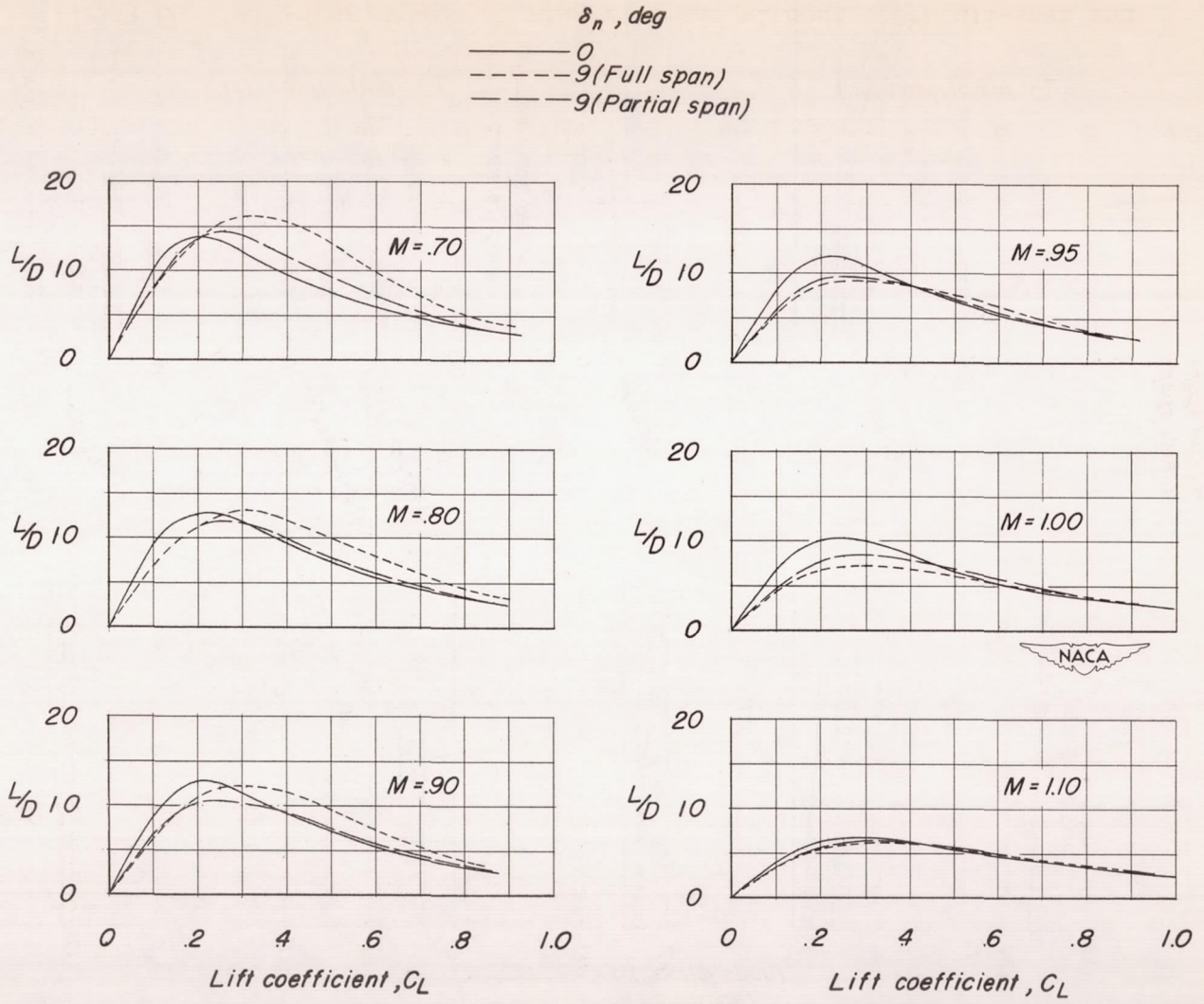

Figure 10.- Lift-drag ratios of wing with and without 9.0° full-span and partial-span leading-edge-flap deflections.

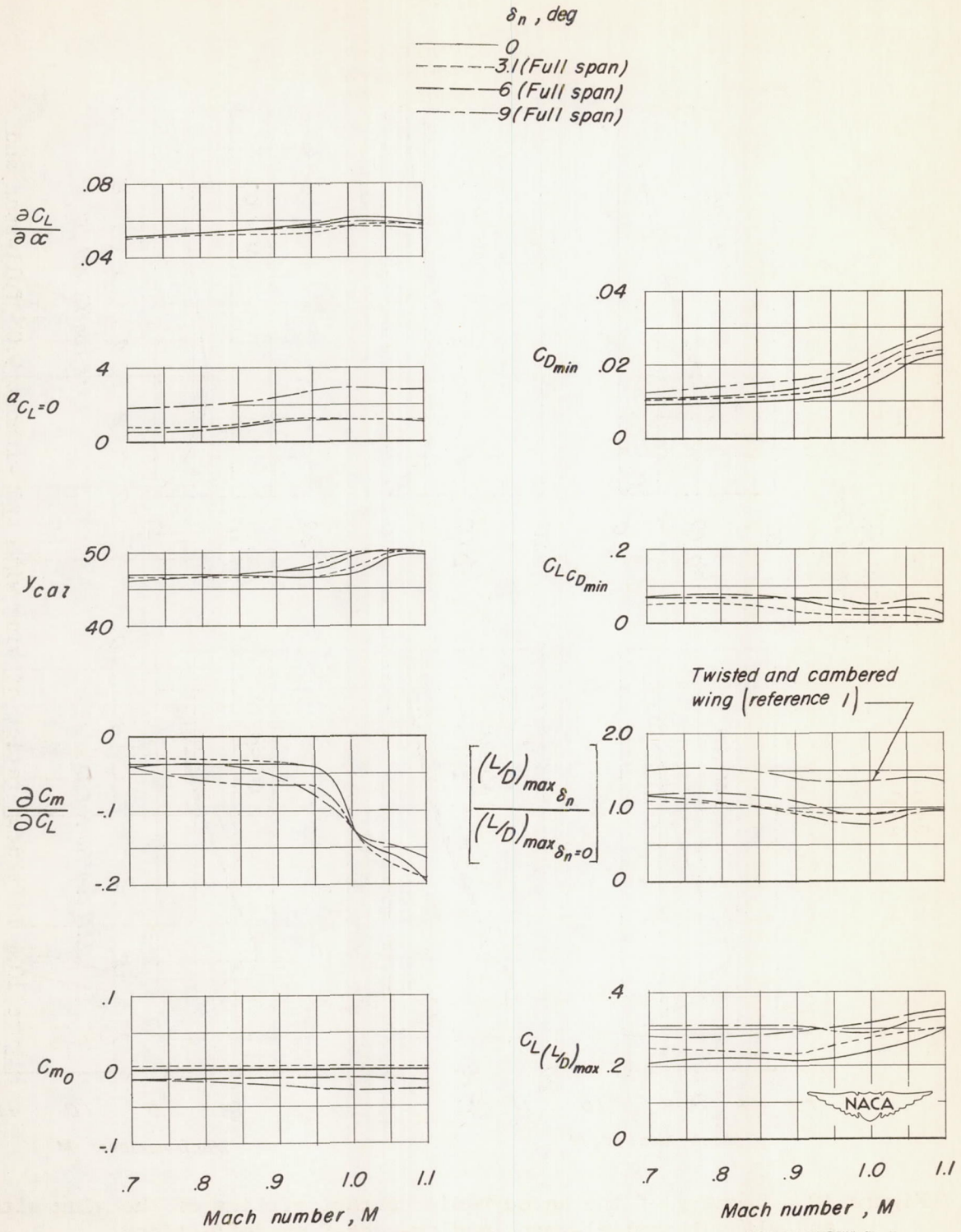

Figure 11.- Summary of the aerodynamic characteristics of the wing with and without full-span leading-edge-flap deflections.

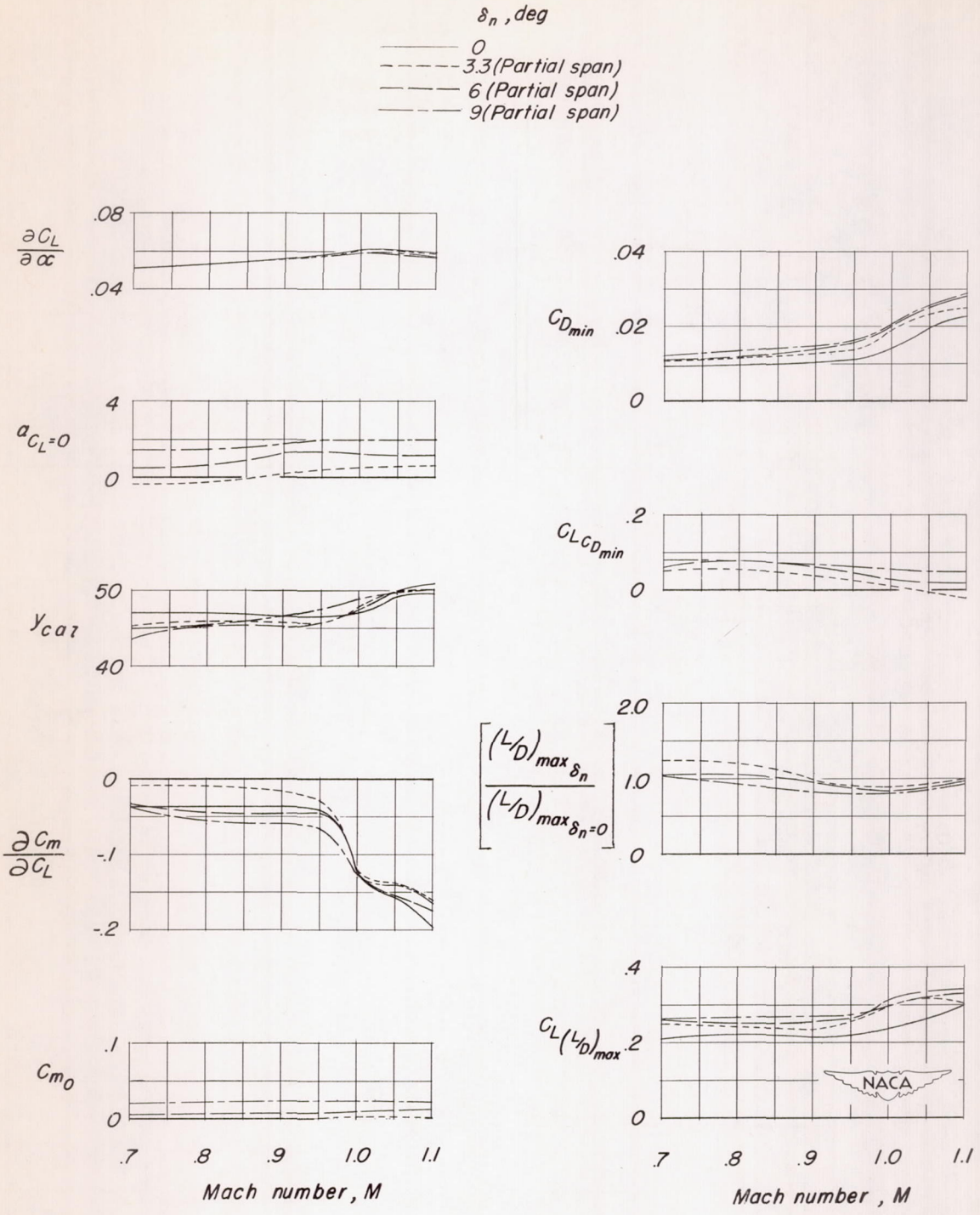

Figure 12.- Summary of the aerodynamic characteristics of the wing with and without partial-span leading-edge-flap deflections.